High-Resolution Estimation of Near-Subsurface Water Content using Surface GPR Ground Wave Information

Susan Hubbard [1], Katherine Grote [2], Michael B. Kowalsky [2], and Yoram Rubin [2]

[1] Lawrence Berkeley national Laboratory, Berkeley, CA 94720 sshubbard@lbl.gov

[2] Dept. of Civil and Env. Engineering, UC Berkeley, Berkeley, CA 94720

1. Introduction

Information about near surface soil water content is a vital component for vadose zone, agricultural and ecological studies, as well as for climate models that require input about processes at the air-soil interface. Our research focuses on investigating the applicability of a surface geophysical method, ground penetrating radar (GPR), for use as a water content estimation tool. To test the potential and benefit of GPR methods under natural field conditions, we have developed a field site at the Robert Mondavi Winery in Napa, CA. The volume and frequency of water application within the vineyards is important for optimizing crop yields, achieving high irrigation efficiencies, minimizing lost yield due to waterlogging and salinization, and achieving maximum vine performance and fruit quality. California uses the largest volume of water of any state in the nation, and as vineyards consume more rural acreage, competition for water resources is increasing. As a result, water content information is also necessary to ensure that surface water supplies do not degrade in water-scarce agricultural areas. Conventional measurements of water content (such as from time domain reflectometry [TDR], neutron probe or gravimetric techniques) are intrusive and provide information at a 'point' scale, which is usually insufficient for managing a crop. Remote sensing data can provide information over much larger spatial areas in a rapid manner. However, it still is a challenge to obtain information about soil water content from the data in the presence of a crop cover (Pultz et al., 1990) such as agricultural areas. At the scales of space and time necessary to describe dynamic vineyard environments, reliance on only sparse, high-resolution point samples or on coarser remote sensing proxy information could generate large uncertainties when used as input to precision farming decisions. Incorporation of water content information potentially available from GPR methods could lead to improved crop management decisions. Similarly, dense and accurate information about water content could lead to improved vadose zone and climatic models.

Our research involves careful development and application of GPR data acquisition and analysis techniques under a variety of hydrological/geological conditions. Our study involves analysis of GPR data and comparison of interpreted information with measurements collected from conventional water content techniques, as well as with soils and remote sensing imagery data. Other researchers have also recognized the potential of GPR as a tool for obtaining information about water content (Du and Rummel, 1994; Chanzy et al., 1996; Greaves et al., 1996; Van Overmeeren et al, 1997, Hubbard et al., 1997; Berktold et al., 1998; Weiler et al., 1998; Lesmes et al., 1999; Huisman et al., 2000;). However, to our knowledge, no study to date has acquired and analyzed spatially dense, high resolution near surface GPR data over an entire field study area and over time, analyzed the travel time and amplitude of such data to obtain a three dimensional volume of temporal water content estimates, and compared such data with dense remote sensing imagery and conventional measurements as we are poised to do in this study. Our overall project goal is to develop GPR interpretational techniques for providing volumetric water content information, and to assess the potential and limitations of this method as a field tool. Here, we discuss a single aspect of the investigation involving use of ground wave GPR data collected at a single central frequency to estimate near surface volumetric water content over our field site.

2. Data Description

Several different types of data were collected at our Mondavi Study site, including water content measurements from conventional point sample tools, soils data, surface and crosshole GPR, and remote sensing imagery. In this section, we briefly describe the parameters of these different data sets.

Point Water Content and Soils Measurements. Conventional water content measuring techniques, including gravimetric, TDR, and neutron probe, were all used to assess water content at the Mondavi Site. These techniques provide only either point measurements over some finite support scale (gravimetric, TDR) or a series of point measurements along the length of the borehole (neutron probe). Both TDR and neutron probe methods require a calibration equation to convert the raw data into estimates of water content. In this study, these conventional water content measurements were used to aid in development of petrophysical relationships for the site and to validate the estimates of water content obtained from the GPR data. Soils data were also collected at 1-foot intervals over 10 feet in all boreholes. The non-gravel portions of the samples were analyzed to determine percent sand, silt and clay. These percentages were converted into soil texture indices with the soil textural triangle used by the U.S. Department of Agriculture and U.S. Soil Conservation Service. The textures were then coded using indicator values of 1-8, where the smaller values represented finer soils and the larger values represented coarser soils.

Remote Sensing Data. Remote sensing data were also collected at the Mondavi site (Johnson et al., 1996) and are being used in this study to compare with information available from soils and GPR data. The remote sensing data were acquired using airborne ADAR Multispectral System 5500 (Positive Systems) collecting in the blue, green, red and near-infrared portions of the spectrum from flight altitude of 4300 m above ground level and with a spatial resolution of 2m x 2m. The operating frequency used in this system is higher than those microwave systems typically employed to map soil moisture in areas of sparse land cover. As plants photosynthetically absorb radiation, remote-sensing systems operating in these frequencies can instead be used to estimate vegetation density, or vigor. The response of the vegetation can be quantified using atmospherically corrected reflectances in the red and near-infrared portions of the spectrum (Rouse et al., 1973; Tucker, 1979) to yield Normalized Difference Vegetation Index (NDVI) values ranging between -1 and 1. Pattern classification analysis algorithms (i.e., Duda and Hart, 1973) can then used with the NDVI values to assign vegetation classifications to the data. The NDVI imagery indicates areas of weak (lower NDVI values) and more vigorous (higher NDVI values) vegetation.

GPR GPR is a geophysical tool that has become increasingly popular as researchers across a variety of disciplines strive to better understand near-surface conditions. GPR uses electromagnetic energy at frequencies of 50-1500 MHz to probe the subsurface. At these frequencies, dielectric properties, characterized by the separation (polarization) of opposite electric charges within a material subjected to an external electric field, dominate the electrical response [Davis and Annan, 1989]. In general, GPR performs better in unsaturated coarse- or moderately coarse-textured soils; GPR performance is often poor in electrically conductive environments such as those dominated by clays. A GPR system consists of an impulse generator, which repeatedly sends a pulse of fixed voltage and frequency spectrum to a transmitting antenna. A signal propagates from the transmitting antenna through the earth and is reflected, scattered, and attenuated by subsurface dielectric contrasts; the receiving antenna subsequently records the modified signal. Figure 1 illustrates the typical energy arrivals recorded by the GPR receiver (Rx) from a transmitter (Tx), where A is the path that the energy takes in air between the transmitter and receiver, G is the path of the ground wave travelling in the near subsurface along the air-ground interface, and R is the path of the reflected event from an interface between materials having different dielectric constant values. Common-offset GPR acquisition entails keeping the distance between the transmitter and receiver constant as the unit is moved along the ground surface; this acquisition mode facilitates rapid data acquisition at walking speed. However, to identify which arrivals are associated with the air, ground and reflectors, it is prudent to also collect "CMP" gathers, whereby the transmitter and receiver are separated at increasingly larger distances about a fixed common midpoint. CMP gathers are laborious to collect, but need only be performed a few times per survey to enable event identification on corresponding common-offset data collected during the same acquisition campaign. Figure 2 displays a portion of a common-offset profile (left) with a nearby CMP profile (right). With both common-offset and CMP acquisition, data are typically displayed as wiggle-trace profiles, with distance on the horizontal axis and signal travel time (one-way travel time for ground waves and two way travel time for reflected events) on the vertical axis. The variations in arrival time, amplitude and phase of the signals indicate subsurface variations in electromagnetic properties. The travel time of the signal can be converted into velocity (V) if the distance of the travel path is known or can be estimated. For example, by picking the arrival time of the air wave (corrected for onset delay) and the ground wave, and then calculating the difference between the two (Δt), we can calculate the velocity of the ground wave (V_{gw}) if we know the separation distance associated with the transmitter and receiver (S, see Figure 1):

$$V_{gw} = \frac{S}{\Delta t}. \tag{1}$$

At the high frequencies used for surface GPR acquisition (~50-1500 MHz), and in geological environments amenable to radar acquisition, the electromagnetic wave velocities (V) obtained from radar data (from analysis of either ground waves or reflected waves) can then converted to dielectric constants (k) using an approximation for low-loss materials:

$$k \approx \left(\frac{c}{V}\right)^2, \tag{2}$$

where c is the speed of light in a vacuum (3×10^8 m/s). Note that this conversion is also used with the measured TDR velocities to obtain estimates of dielectric constants.

Dielectric constants (κ) vary as a function of water content, porosity, operating frequency, lithology, temperature, and pore fluid composition. Water content, however, typically has the greatest influence on the measured dielectric constant of the soil. The dielectric constant of air is 1, of water is 80, and of dry natural geologic materials (with air in pore spaces) is approximately 3-8; addition of water to the soil pore space drastically increases the dielectric constant and thus alters the GPR response. Petrophysical models are necessary to link dielectric constant estimates, available from TDR or GPR data, to water content. These petrophysical relationships can be developed for the specific site of interest or can be borrowed from literature. For example, Topp et al. (1980) developed a regression analysis between dielectric constant and volumetric water content (θ) of many soils having different textures:

$$q = -5.3\times10^{-2} + 2.92\times10^{-2}\,k - 5.5\times10^{-4}\,k^2 + 4.3\times10^{-6}\,k^3. \tag{3}$$

Although empirical, the 'Topp relationship' has been widely used by soil scientists for converting measured dielectric constant values (from TDR) into estimates of volumetric water content.

In this study, we present information obtained by analysis of ground wave data collected at a single central frequency of 900 MHz. The zone of influence of this data is approximately the top 9 cm below the ground surface. For the ground wave analysis, data processing was minimal and included bandpass filtering and minimal amplitude balancing. Further analysis of the travel time and amplitude information obtained from ground wave data collected using lower frequency antennas, as well as from deeper reflected events, are underway and will be presented at a later date.

3. Ground Wave Investigations at the Mondavi Field Site

The Robert Mondavi Field site is located next to the Robert Mondavi Winery near the town of Oakville in Napa County, California. Figure 3 shows the location of the field site relative to the San Francisco Bay Area in California, and illustrates the field site layout. The field site layout is superimposed on top of NDVI imagery collected in August of 1998; in this image the brown color is indicative of weak vegetation and the green signifies more vigorous vegetation. Our study site, outlined by the heavy black line on Figure 3, encompasses areas of both vigorous and weak vegetation over an area of approximately 10,000 square meters. As shown by the field map, many neutron probe access holes have been drilled, cased and logged to characterize subsurface soil and water content information over time. After hole installation and soil sample collection, neutron probe data were collected in each well and soil samples were analyzed for soil texture and gravimetric water content. Full field grids of GPR data, representative CMP gathers, and neutron probe logs at all holes were collected at three different times during a one-year period: June 19, 2000, October 18, 2000, and May 10, 2001. During each of these data acquisition campaigns, GPR lines were collected along every 5^{th} row minimally between rows 35 and 155 (see Figure 3) using a 900 MHz PulseEKKO 1000 system, 10-20 cm station spacing, 100 ps sampling interval, and 32 stacks.

In order to interpret ground wave information in terms of water content, it is imperative to both identify the correct air and ground arrivals (to enable calculation of Δt in (1)), and to establish a relationship between the dielectric constant and water content. The air and ground wave arrivals on the common-offset data were identified by analysis of the CMP data collected during each acquisition campaign. Additionally, small-scale infiltration studies, associated with two different data acquisition campaigns, were performed to better understand the ground wave responses to increased water content. In these infiltration studies, GPR data were collected prior and subsequent to introduction of water. As the moisture increased, the ground wave travel time increased. As a result, the ground wave arrived later in time relative to the air wave, which facilitated identification of the ground wave signature and a better understanding of the superposition of portions of the air and ground wave under dry conditions. GPR and TDR data collected during the infiltration studies were also used to determine the ground wave travel path distance ("S") used in Equation 1. In our case, the emitted pulse of the PulseEKKO antennas is radiated partially from the center and partially from the ends of the transmitting antenna, and thus the separation distance value used is slightly greater than the distance between the midpoints of the transmitting and receiving antennas. By calibration of the groundwave travel times with TDR measurements collected over a variety of water content values, a value of 21 cm was obtained for the 900 MHz antennas "S" value.

We developed relationships between neutron probe backscatter counts and volumetric water content using co-located neutron probe and gravimetric water content measurements and assuming a soil density value; these relationships enabled us to convert our neutron probe logs into volumetric water content. Crosshole radar data were also collected between selected wells to provide detailed information about velocity variations in the vertical direction between the wells. Zero-offset crosshole radar data acquisition entails transmitting energy from an antenna located in a wellbore to a receiving antenna located in another wellbore at the same depth (Peterson, 2001). Since the travel distance is known (the wellbore separation) and the travel time of the transmitted signal can be picked from the data, the electromagnetic velocities can be calculated as a function of depth. Using 200 MHz cross-hole radar velocity measurements, equation (2), and neutron probe backscatter counts collected in the same boreholes and interpreted in terms of volumetric water content, we developed a relationship between dielectric constant and volumetric water content for our site. Our developed site-specific relationship turned out to be very similar to the relationship given by Topp et al. (1980) in Equation (3). As such, all following estimates of water content from dielectric constant measurements will invoke the established Topp et al. (1980) relationship to convert GPR estimates of dielectric constant into volumetric water content estimates.

Analysis of the travel times of ground wave data collected at the Mondavi site was performed to assess near-surface variations in volumetric water content over space and time. The arrival times of the air and ground waves from the GPR data were picked and compensated for zero-time starting delays. The travel times were converted into velocities using (1) with a distance (S) associated with the antenna separation for our system as discussed above. The velocity values were in turn converted into dielectric constants using (2) and then into volumetric water content using (3). Figure 4 gives an example of estimates of water content obtained with this method using 900 MHz ground wave travel time data collected May 2001 along two selected lines with a station-sampling interval of 10 cm. The scatter observed in the estimates are suspected to be due to the picking inaccuracies, inaccurate assumptions in the ground wave travel path, or use of the simple Topp relationship for converting from dielectric constant to water content (Equation 3) without considering the influence of soil texture. Polynomial fitting of the GPR estimates enables visualization of the more general trends in water content along these rows. TDR data were also collected during the May 2001 campaign and included a grid of 66 TDR measurements along selected GPR lines using 15cm TDR probes. Figure 4 also illustrates the water content values from the TDR measurements collected along the selected rows, as well as a fit to those data using the same order polynomial as was used to fit the GPR data. Comparison of the GPR and TDR fitted lines suggests that the GPR estimates of water content have similar trends to the TDR measurements made along the same line, and also have similar ranges of volumetric water content. The observed differences between the GPR estimates and TDR measurements may be attributable to the GPR inaccuracies as discussed above, the differences in measurement frequency as described by Weiler et al. (1998), the difference in support volume and depth of influence of the GPR and TDR, as described by Huisman et al. (2001), or to TDR measurement errors caused by, for example, the presence of an air gap around the probes. Nonetheless, line-by-line comparison of the TDR and GPR water content estimates, such as those shown in Figure 4, as well as two-dimensional contour plots of the TDR measurements and GPR estimates of volumetric water content over the entire study area reveal consistent water content ranges and spatial patterns. The similarities give us confidence that the GPR is providing spatially dense and potentially valuable information about the near surface water content at our field site.

Using the same approach described above, we investigated the ground wave arrivals collected during other data acquisition campaigns. Figure 5 shows the estimated water content from other 900 MHz GPR data collected along R145 at other times throughout the year. This figure suggests that there are temporal changes in the mean water content along this row with time, but that the location of the volumetric content maximum and minimum seems to be relatively fixed in space and may be controlled by near surface soil texture. Extending the ground wave analysis into two-dimensional space, Figure 6 illustrates the variations in water content in the very near surface estimated for the May 2001 grid obtained from analysis of the 900 MHz ground wave data over the entire study area. Preliminary analysis of the GPR grids collected during the June 2001 as well as the October 2001 campaigns suggest that there is a spatial persistence of water content patterns and that the water content patterns seem to be influenced by near-surface soil texture, precipitation and irrigation. Additionally, we are investigating the influence of soil texture on water content estimates, and of water content estimates on the NDVI imagery. A comparison of the water content estimates obtained from GPR (Figure 6) with the soils and NDVI imagery (for example, the NDVI image in Figure 3) preliminarily suggests that the dryer areas are associated with the areas of coarser grained near-surface soils and also with the most vigorous vegetation.

4. Conclusions and Future Research

No technique can currently provide high resolution soil water content information quickly, reliably, and at low cost. Estimation of water content using 900 MHz ground wave travel time data was shown to yield high-resolution information about volumetric content for the very near surface. Comparison of the GPR-obtained estimates with conventional measurements of water content suggests that the GPR approach provided useful information about water content in a much more spatially dense and non-invasive manner relative to the conventional techniques. Analysis of the time-lapse surface GPR data is underway, as well as a quantitative comparison of the GPR-obtained water content information with information available from soils and remote sensing data. Additionally, analysis of the spatial correlation of the different types of data is underway to investigate the spatial correlation functions obtained from the different types of data sets, the seasonal change in water content spatial correlation using the GPR-obtained estimates and the improvement in the estimation of the spatial correlation function when GPR data are included in the analysis. Finally, we will also include information available from travel times and amplitudes of lower frequency ground wave information and reflected energy into the estimation to obtain a high-resolution, 3-D volume of GPR-obtained water content estimates as a function of time. Successful development of GPR interpretation techniques could facilitate rapid and accurate acquisition of water content information, which in turn may lead to improved precision vineyard management and vadose zone models, increased water savings, reduced energy expenditures, and better control on the ecology of natural vegetation.

5. References

Berktold, A., K.G. Wollny, H. Alstetter, 1998, Subsurface moisture determination with the ground wave of GPR, GPR 98 Conference.

Chanzy, A., A. Tarussov, A. Judge, F. Bonn, 1996, Soil water content determination using a digital ground-penetrating radar. *Soil Science Society of America Journal* 60, 1318-1326.

Du, S. and P. Rummel, Reconnaissance studies of moisture in the subsurface with GPR, IN: Fifth international conference on GPR, Waterloo Center for Groundwater Research, Waterloo, Kitchener, Ontario, Canada, p. 1241-1248, 1999.

Duda, R. and Hart, P., 1973, Pattern Classification and Scene Analysis, John Wiley and Sons Inc., New York, NY.

Greaves, R.J., Lesmes, D.P., J.M. Lee, M.N. Toksoz, Velocity variations and water content estimated from multi-offset ground penetrating radar, *Geophysics* 61, 683-695, 1996.

Hubbard, S.S., Y. Rubin and E. Majer, 1997, Ground Penetrating Radar for Saturation and permeability Estimation in bimodal systems, *Water Resources Research*, 33, p. 971-990.

Huisman, J.A., C. Sperl, W. Bouten, J.M. Berstraten, 2000, Soil water content measurements at different scales: accuracy of time domain reflectometry and ground penetrating radar, *Journal of Hydrology* 245, 48-58.

Johnson, L., Lobitz, B., Armstrong, R., Balkdy, R., Weber, E., DeBenedictis, J. and Bosch, D., 1996, Airborne imaging aids vineyard canopy evaluation, *California Agriculture*, 15(4), 14-18, 1996.

Lesmes, D.,R.J. Herbstzuber, and D. Wertz, 1999. Terrain permittivity mapping: GPR measurements of near-surface soil moisture, in proceedings on the application of geophysics to engineering and environmental problems, EEGS, p. 575-582. Oakland, CA, March 14-18, 1999.

Peterson, J., 2001, Pre-Inversion Corrections and analysis of radar tomographic data, Journal of Environmental and Engineering Geophysics, 6(1), 1-18.

Pultz, T.J., R. LeConte, J. Brown and B. Brosco, Quantitative soil moisture extraction from airborne SAR data, *Can. J. Remote Sens*. 16, 56-62, 1990.

Rouse, J.W., Haas, R.W., Schell, J.A. and Deering, D.W., 1973, Monitoring vegetation systems in the great plains with ERTS, Third ERTS Symposium, NASA, SP-351, volume 1, 309-317.

Topp, G.C., Davis, J.L, Annan, A.P., 1980. Electromagnetic determination of soil water content: measurements in coaxial transmission lines. *Water Resources Research* 16(3), 574-582.

Tucker, C.J., 1979. Red and photographic infrared linear combinations for monitoring vegetation. *Remote Sensing of the Environment*, 8: 127-150.

Van Overmeeren, R.A., S.V. Sariowan, J.C. Gehrels, 1997, Ground penetrating radar for determining volumetric soil water content: results of comparative measurements at two sites. *Journal of Hydrology*, 197, 316-338.

Weiler, K.W., T.S. Steenhuis, J. Bull and K.-J.S. Kung, 1998. Comparison of ground penetrating radar and time domain reflectometry as soil water sensors, *Soil Science Society of America Journal* 62, 1237-1239.

Acknowledgements

This study was funded by WRC project W-929, NSF EAR-0087802, and USDA 2001-35102-09866 to Yoram Rubin. We sincerely thank Daniel Bosch and the Robert Mondavi Winery for providing vineyard technical information and access as well as in-kind support, and Lee Johnson (CSU Monterey Bay and NASA/Ames Research Center) for providing access to the remote sensing imagery.

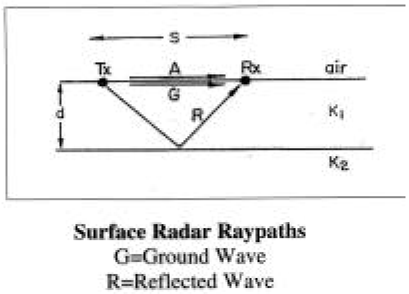

Figure 1. Schematic illustrating air, ground wave, and reflected GPR energy travel paths. S is the separation distance between the transmitter (Tx) and receiver (Rx).

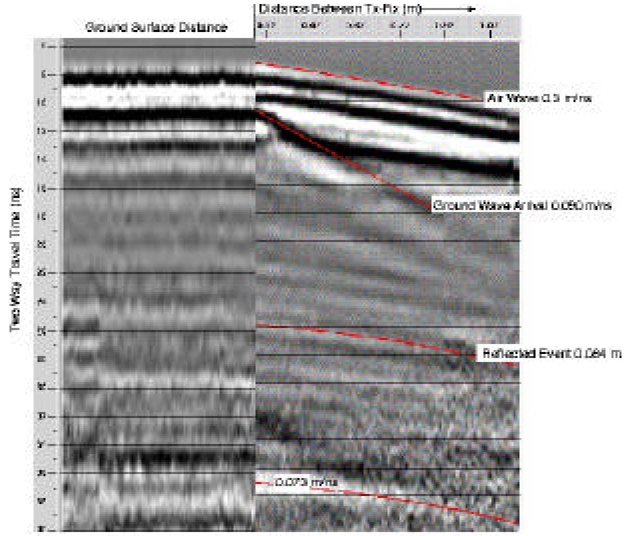

Figure 2. Comparison of GPR common offset Profile (left) with nearby GPR CMP gather (right)

Figure 3 Location and layout of Mondavi Field Study Area.

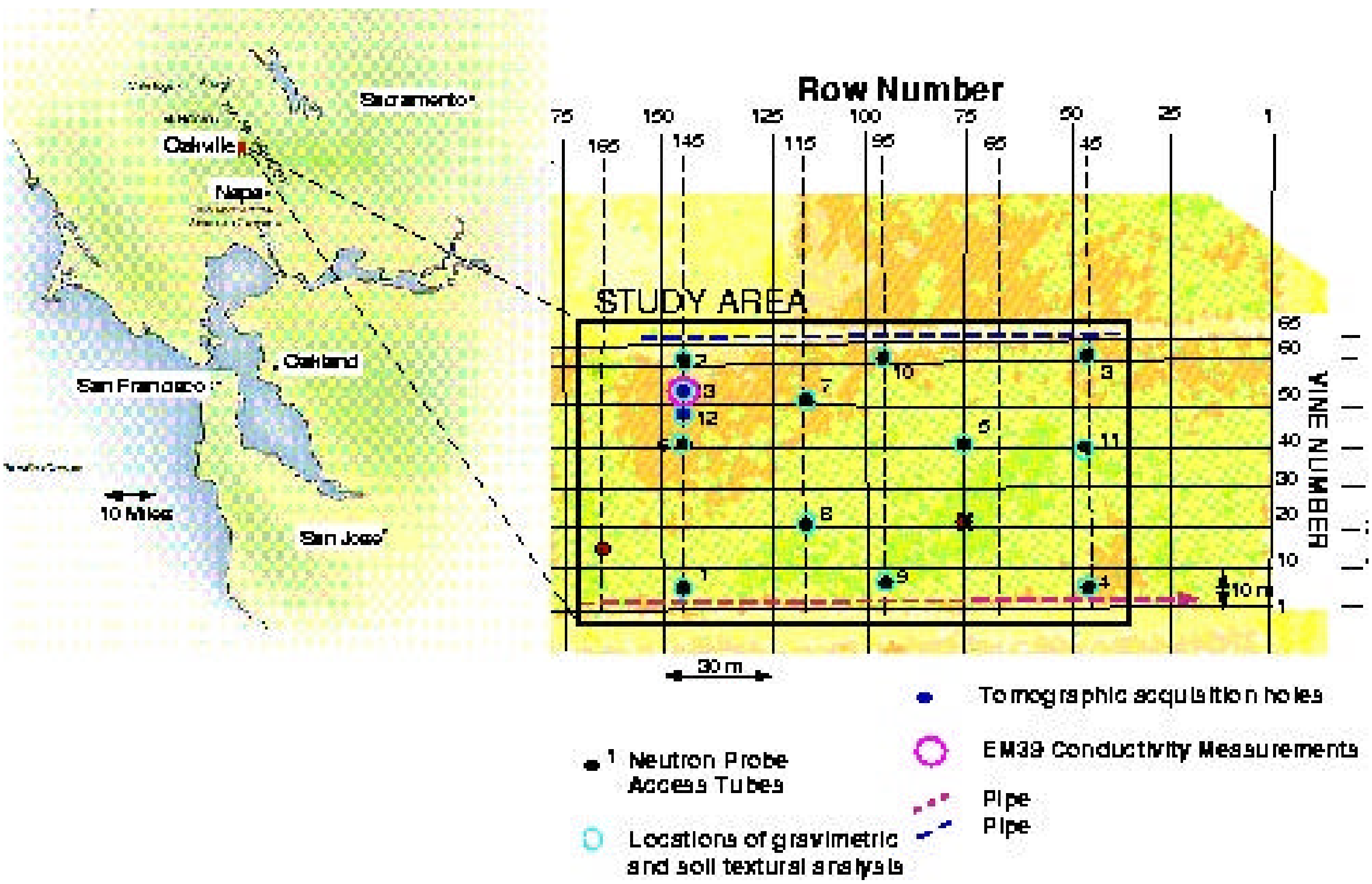

Figure 4. Comparison of GPR and TDR values and fitted lines along selected rows.

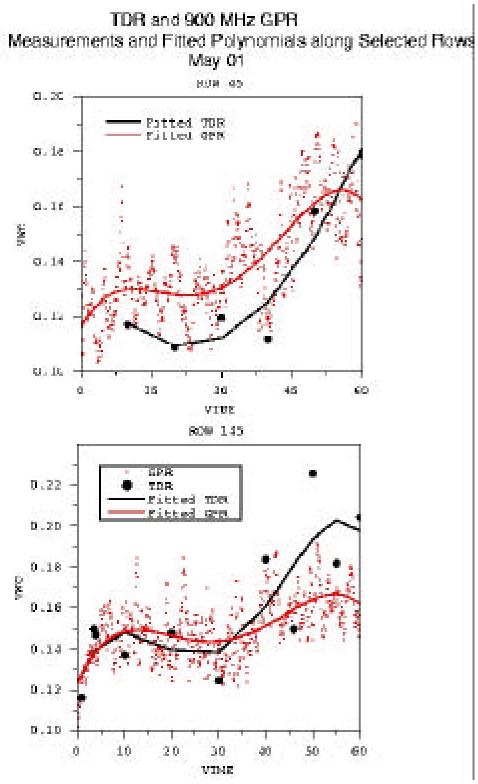

Figure 5. Spatial and temporal variations in water content estimated from GPR ground wave travel time data along a single vineyard row.

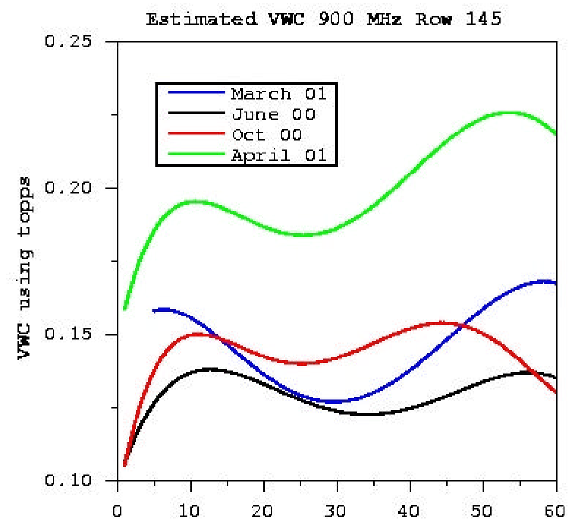

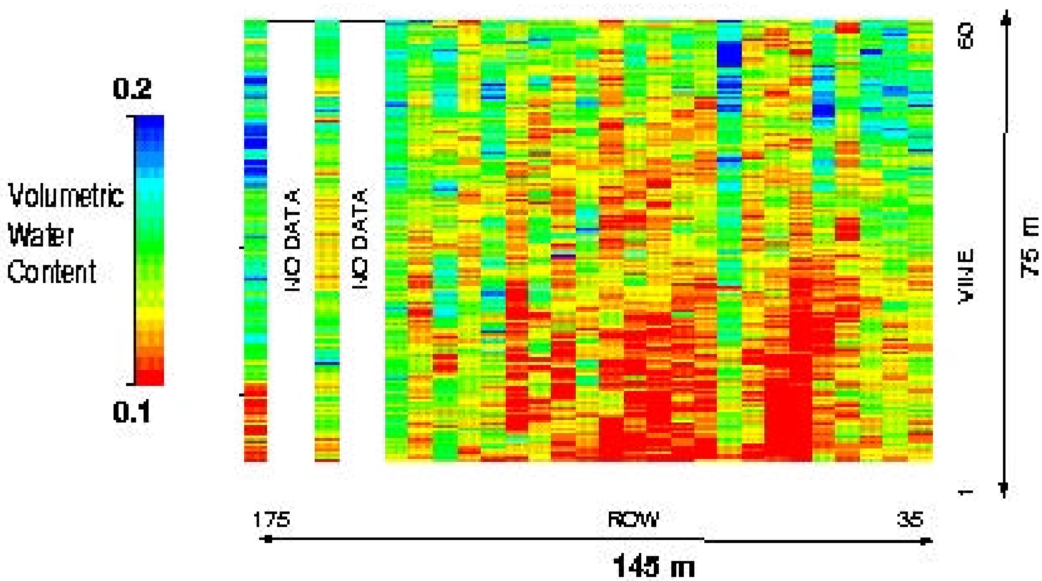

Figure 6. Estimates of volumetric water content (VWC) obtained from 900 MHz GPR data collected during the May 2001 acquisition campaign over the entire study site. Sampling interval along the rows is 10 cm, and GPR lines were collected every 5th Row.